NEW DRAG REDUCTION METHODS FOR TRANSPORT AIRCRAFT

G. Löbert

MBB Military Aircraft Division

Munich, Germany

Abstract

The following methods of drag reduction are described and their effectiveness is assessed.

- Active boundary layer thickening

  It is well known that the skin friction coefficient of a turbulent boundary layer varies inversely as the one-fourth power of the boundary layer thickness. If the fuselage boundary layer is artificially thickened by a wind turbine mounted at the fuselage nose and the turbine power is transferred to a propeller mounted at the aft end of the fuselage, it should be possible to reduce the cruise fuel requirement of current transport aircraft by about 8%.

- Low-pressure jet mixing

  The thrust minus drag of a jet engine/wing combination can be increased considerably if measures are taken that provide intensive jet mixing in the region of negative pressure above the lifting wing. With a proper choice of engine location and nozzle geometry, a reduction in cruise fuel in excess of 7% should be attainable.

- The propulsive wing

  It should be possible to recover most of the profile thickness and camber drag by exhausting the propulsion stream through a linear array of slot nozzles into the upper surface boundary layer immediately ahead of the pressure recovery region. Cruise fuel requirement could be reduced by some 5%.

- Multiply bifurcated wing tips

  It is shown that for a given wing weight only the symmetrically pronged wing tip can reduce vortex drag. For a wing bifurcated at 80% semi-span into a two-pronged tip of $\pm$ 45° dihedral angle, vortex drag is reduced by 5.6% relative to the plane wing of equal weight. Bifurcation of the tips of the two winglets reduces vortex drag by an additional 3.2%, thus reducing the cruise fuel requirement by some 3%.

- Freely floating tip vortex sails

  With free floating, geared wing tip vortex sails it should be possible to recover over 10% of the wing vortex drag with little additional loading of the wing.

By combining all five concepts it should be possible to reduce the fuel burn of current turbo-fan powered transport aircraft by some 20%.

1. Introduction

Reduction of drag has always been one of the prime objectives of aeronautical research, since no other single quantity influences the operating costs of transport aircraft more than aerodynamic drag. The dramatic increase in fuel price that occurred in the last decade has further emphasized the importance of this subject. The purpose of this paper is not to provide a comprehensive review of recent developments in the field of drag reduction, but to present some novel drag reduction methods proposed by the author in the last few years and to assess their probable effectiveness. These methods pertain to the reduction of skin friction drag, vortex drag and the interference drag between the wing and the propulsion jets.

2. Reduction of Skin Friction Drag by Active Boundary Layer Thickening

If four flat plates of equal size are placed one behind the other in a uniform high-speed flow, a simple calculation shows that the aft plate experiences a drag force that is smaller than that of the forward plate by some 38%. This lower drag stems from the fact that for a turbulent boundary layer, the wall shear stress varies inversely proportional to the fourth root of the boundary layer momentum thickness. If it were possible to increase the boundary layer momentum thickness by a factor of 4, skin friction drag could be reduced by 30%.

Boundary layer thickening by passive means is, of course, entirely ineffective, because the pressure drag associated with the thickening device exceeds the skin friction drag reduction by far. In contrast, overall drag can be reduced considerably if the boundary layer is thickened by active means. In this case, a highly efficient wind turbine, mounted in front of the fuselage, is used to increase the momentum thickness of the fuselage boundary layer.

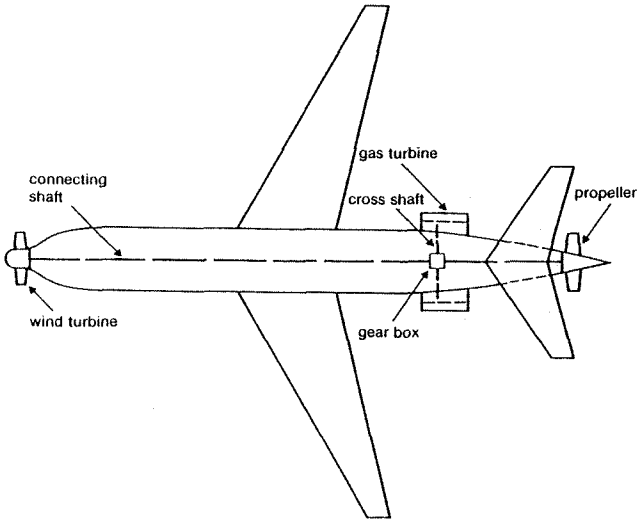

Fig. 1 Implementation of the concept of active boundary layer thickening

By means of a connecting shaft, the output power of the turbine is transmitted to a propeller mounted at the aft end of the fuselage, where it is converted into a thrust force. The blade settings of both devices are selected such that at the desired shaft r.p.m. turbine power is equal to propeller power plus transmission losses. In this condition turbine drag plus fuselage drag minus propeller thrust is considerably less than fuselage drag without boundary layer thickening, as is shown in Ref. 1. Note that the swirl of the turbine opposes that of the co-rotating propeller.

Once installed, the stern propeller can, of course, additionally be used to propel the aircraft in combination with two turboprop power plants installed on the wing. The ground clearance problem, which is present during take-off, could be solved by selecting a large flap angle in order to reduce the pitch attitude at lift-off.

The concept of active boundary layer thickening is analyzed in detail in Ref. 1.

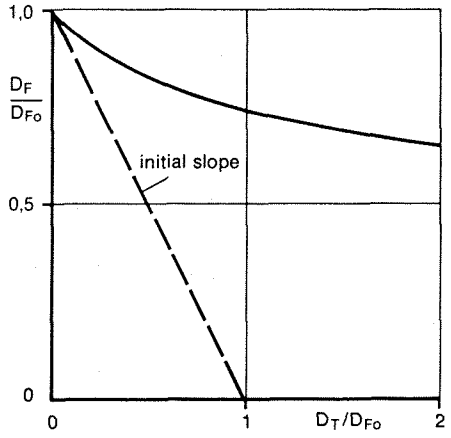

Fig. 2 Influence of windmill drag on fuselage skin friction drag

Fig. 2 shows the variation of fuselage drag with turbine drag. Fuselage drag initially decreases rapidly with increasing boundary layer thickening. As D_T/D_{F_O} increases further, the slope of the curve decreases steadily. In contrast, the losses incurred in the turbine and the propeller increase almost linearly with turbine drag. Thus there exists an optimum value of the ratio of turbine drag to fuselage drag at which the power required to propel the fuselage plus the turbine, transmission and propeller losses, is a minimum.

As is to be expected, the effectiveness of active boundary layer thickening depends strongly on the efficiency of the wind turbine and of the propeller as well as on the power transmission losses. On the other hand, the concept gains a large benefit from the fact that the thrustor is located in the low velocity region at the aft end of the fuselage.

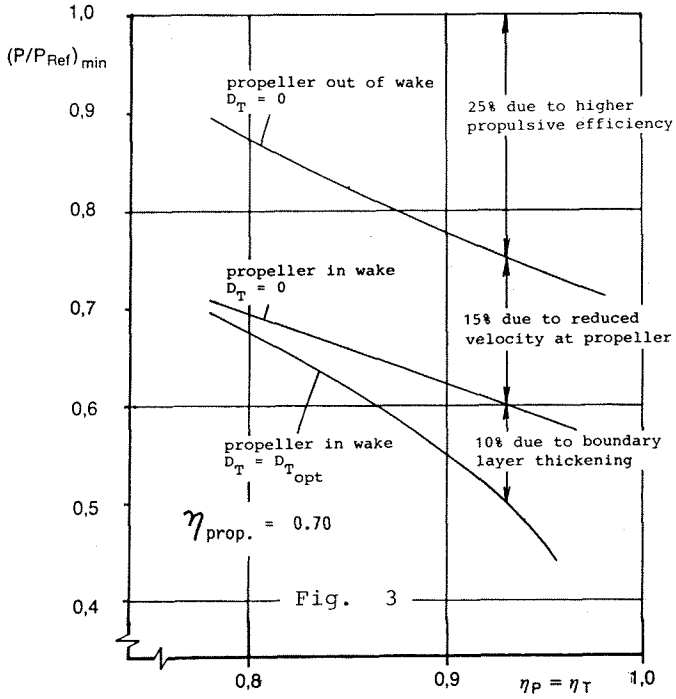

Fig. 3

Fig. 3 shows the ratio of the power required to propel the turbine/fuselage/propeller combination to the propulsion power requirement of a conventional fuselage of equal size, propelled by a turbo-fan engine, as a function of the efficiencies of the wind turbine and the propeller. The propulsive efficiency of 70% used for the reference aircraft is characteristic of advanced high by-pass-ratio turbo-fan engines (see Ref. 2). For a turbine/propeller efficiency of 90%, which corresponds to the state of the art 40 years ago, the necessary fuselage propulsive power can be reduced by approximately 45% relative to that of a fuselage propelled by a separate turbo-fan engine. The higher propulsive efficiency of the propeller relative to that of the turbo-fan engine provides 22% reduction. The reduced inflow momentum to the propeller adds another 16% improvement, and the concept of active boundary layer thickening provides a further power reduction of 7%. The power reduction resulting solely from the novel turbine/propeller installation amounts to 28%. In view of the assumptions made in the analysis, the latter value can be considered to be conservative.

With modern airfoil technology, the wind turbine/propeller efficiency could be increased by some 3%, thereby increasing the effectiveness of active boundary layer thickening further. Alternatively, this advanced technology could be used to reduce the speed gap between propeller-driven transports and turbo-fan aircraft to approximately 15%. In this case it may be beneficial to install a small number of swirl-inhibiting vanes on the fuselage.

It is estimated that for long-range transports, the weight of the wind turbine and the power transmission hardware is only a small fraction (typically 15% - 20%) of the weight of the fuel saved by active boundary layer thickening. Considering that the sensitivity of direct operating costs to block fuel is two to three times higher than the sensitivity with respect to operating weight empty (3) and that this ratio increases steadily as oil becomes scarcer, the weight penalty of active boundary layer thickening is of minor importance in comparison to the fuel saving potential of this concept.

3. Drag Reduction by Means of Low-Pressure Jet Mixing

Wind tunnel tests with jet engine simulators have shown that the location of the engine relative to the wing has a strong influence on the resultant thrust minus drag of the combination (4). It is generally found that nacelles located below the wing plane provide an unfavorable jet/wing flow interaction, while the reverse holds for over-the-wing engine installations.

In Ref. 5 the drag interference between a wing and a jet discharging into the low-pressure field above the wing was analysed and a physical explanation was given for the observed thrust augmentation.

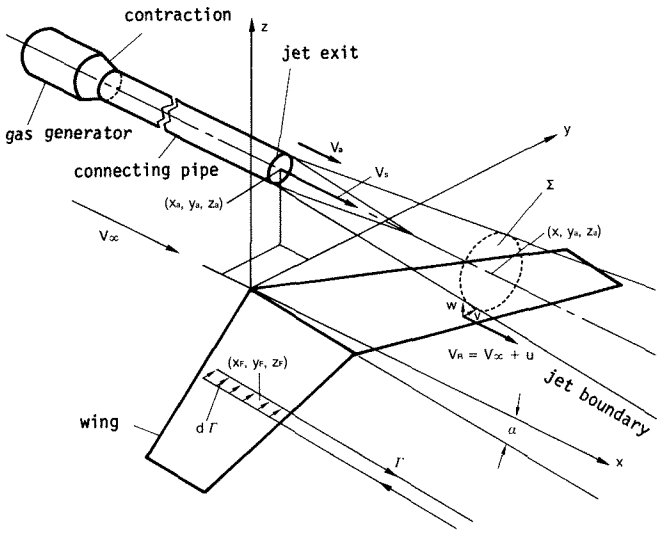

Fig. 4 Simplified flow model used to study jet/wing drag interference

Fig. 4 shows the simplified model of Ref. 5.

A first hint at the origin of the additional propulsive force is obtained if the jet/wing-combination is viewed as an ejector with a single-sided shroud. The full explanation follows, if one realises that the mixing jet produces an upwash at the wing, which requires a corresponding change in slope of the wing surface, if the original pressure distribution is to be maintained. As a result of this slope change, all pressure forces are tilted forward with a subsequent reduction in wing drag. Oddly enough, this drag reduction manifests itself in the Trefftz plane as an increase in jet momentum.

Another peculiarity of the problem is the fact that the reduction of wing drag can be calculated by integrating the longitudinal velocity induced by the lifting wing on the axis of the jet multiplied by the local jet suction intensity.

To first order, the interference drag reduction is given by

$$\frac{\Delta\,(T-D)}{T} = \frac{u_{eff}}{V_\infty} \cdot F_j \qquad (1)$$

where

$$u_{eff} = \frac{\int u(x)\,\mu(x)\,dx}{\int \mu(x)\,dx} \qquad (2)$$

$$F_j = 1 - \frac{T_j/T_\infty}{V_j/V_\infty} - \frac{\gamma-1}{2} M_\infty^2 \left(\frac{V_j}{V_\infty} - 1\right) \qquad (3)$$

T-D = resultant propulsive force

T = engine net thrust

T_j, T_∞ = static temperature of the gas jet and the ambient air

V_j, V_∞ = jet velocity, freestream velocity

γ = ratio of specific heats

M_∞ = freestream Mach number

u(x) = x-component of the velocity induced by the airframe at the jet axis

$\mu(x)$ = local mixing intensity (sink density) of the gas jet

From the definition of u-eff it can be seen that for maximum thrust augmentation, jet mixing should occur at as high a negative pressure as possible. The shape and location of the jet engine nozzle should therefore be designed in such a way that intensive jet mixing occurs in the region of maximum negative pressure above the wing. Scrubbing of the wing surface by the jet must, of course, be avoided.

Fig. 5a shows a possible arrangement of engine and wing. Strong jet mixing can be achieved with vortex generators (Fig. 5a), lobed nozzles (Fig. 5b), multi-tube nozzles (Fig. 5c) or other devices.

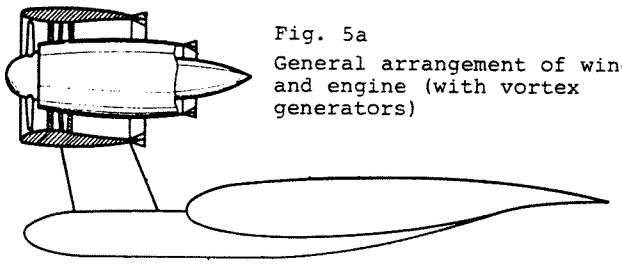

Fig. 5a
General arrangement of wing and engine (with vortex generators)

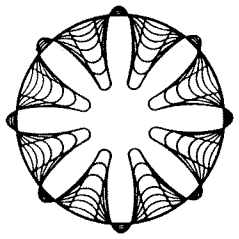

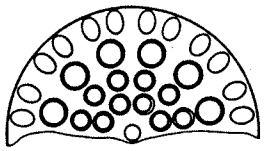

Fig. 5c Multi-tube nozzle

Fig. 5b Multi-lobe hypermixing nozzle

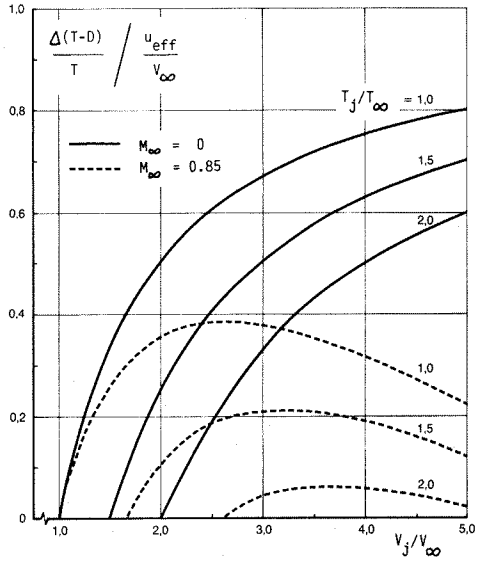

Fig. 6 Influence of jet velocity and temperature ratio as well as freestram Mach number on thrust augmentation

The magnitude of the jet factor Fj is evaluated in Fig. 6 where the relative increase in the resultant propulsive force divided by u-eff/v∞ is shown as a function of the jet velocity ratio for several values of the jet temperature ratio at two different freestream Mach numbers. It can be seen that for imcompressible flow the thrust augmentation increases steadily with increasing velocity ratio. A high jet temperature is unfavourable, especially at low jet velocity ratios. For $T_j/T_\infty > V_j/V_\infty$ the mixing jet displaces the outer flow away from the jet axis, so that drag interference is negative in this case for over-the-wing installations.

Fig. 6 also shows that compressibility of the freestream flow reduces the effectiveness of the concept. For each value of the jet temperature ratio there exists a velocity ratio for which F_j is maximised.

At present it is not possible to accurately calculate the thrust augmentation that can be obtained by low-pressure jet mixing. For one thing the detailed distribution of suction intensity along the axis of hypermixing nozzles is not known. Furthermore, the analysis of Ref. 5 is restricted to subcritical wing flow. The effectiveness of favourable jet/wing interaction can therefore only be assessed in a coarse manner.

In the following paragraphs an upper limit to the possible thrust augmentation is estimated for transport aircraft in cruising flight. The degree to which this maximum thrust augmentation can be exploited can only be determined in wind tunnel tests.

At cruise, transport aircraft with supercritical wing sections exhibit an extensive region of low-pressure supersonic flow above the wing. The wing is usually designed so that over the forward 70% of the wing chord the upper surface Mach number normal to the local sweep line is 1.2 to 1.3. Because of the low upper surface curvature in the supersonic region of super-critical wings the Mach number gradient normal to the wing surface is relatively low, so that for a small vertical spacing between the wing and the jet, the surface Mach number can be assumed to also apply at the jet axis. The longitudinal induction velocity of the wing can then easily be calculate as a function of the normal Mach number M_n, wing sweep angle Λ, and cruise Mach number M_∞.

$$\frac{u_{max}}{V_\infty} = \left[\frac{M_n}{M_\infty} \sqrt{\frac{1+\left[(\gamma-1)/2\right] M_\infty^2 \cos^2\Lambda}{1+\left[(\gamma-1)/2\right] M_n^2}} - \cos\Lambda \right] \cos\Lambda \qquad (4)$$

A second assumption in the determination of the upper boundary to thrust augmentation is that the hypermixing nozzle can be so designed that jet mixing occurs entirely within the local supersonic region at the pressure corresponding to M_n. Clearly, the wing surface has to be deformed extensively, if the essentially shockless supersonic flow is to be maintained under the action of the hypermixing jet. This again has an adverse effect on manufacturing costs and aircraft off-design behaviour. The possible payoff is, however, considerable, as is shown below.

Inserting eq. 4 into eq. 1, one obtains an expression for the upper limit of the thrust augmentation possible with the concept of low-pressure jet mixing.

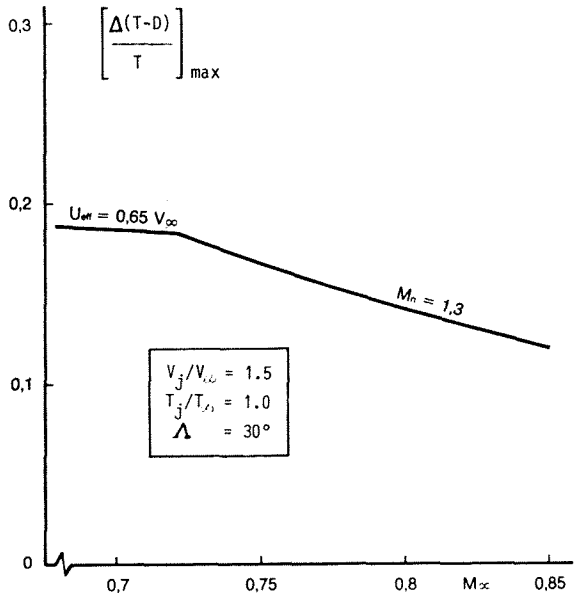

Fig. 7 Maximum thrust augmentation ratio in cruising flight

In Fig. 7 this expression is evaluated for $\Lambda = 30°$, $M_n = 1.3$, $V_j/V_\infty = 1.5$ and $T_j/T_\infty = 1$ as a function of the cruise Mach number M_∞. The above values are characteristic of modern turbo-fan powered transport aircraft. As can be seen, the effectiveness of the concept of low-pressure jet mixing increases with decreasing cruise Mach number because of the steadily increasing value of U_{max}/V_∞. Boundary layer separation sets an upper limit to the maximum upper surface velocity, so that the maximum thrust augmentation remains nearly constant below $M_\infty = 0.72$.

Even if only 50% of the thrust augmentation shown in Fig. 7 can be realised in a practical nozzle/wing design, the concept of low-pressure jet mixing can be considered a highly effective means of increasing the fuel efficiency of transport aircraft.

A further increase of thrust augmentation is obtained at low speeds (for example at the speed corresponding to the second climb segment, which usually sizes the engine) because V_j/V_∞ is higher and M_∞ is lower here. In this speed regime Ewald obtained a thrust augmentation of 20% of the net thrust with a simple circular nozzle (4).

4. The Propulsive Wing as a Means of Drag Reduction

This concept for the reduction of wing drag is based on the following fluid mechanical phenomenon:

An excrescense such as a rivet head located on an airfoil in a region of high velocity ($V_{local} > V_\infty$) increases the drag of this airfoil by an amount that is considerably in excess of the drag this excrescence would experience on a flat plate at a freestream velocity equal to V_{local}. In actual fact the airfoil incremental drag increases with local velocity as

$$\Delta D \sim (V_{local}/V_\infty)^{4.25} \quad (5)$$

This result follows from the drag formula for an airfoil in incompressible flow (6)

$$c_{D_p} = \frac{0.074}{Re^{0.2}}\left[62.5\,(\frac{\delta_2^*}{c})^{1.25} Re^{0.25} (\frac{V_*}{V_\infty})^{4.25} + \int_{\frac{x^*}{c}}^{1} \left[\frac{V(x/c)}{V_\infty}\right]^4 d(\frac{x}{c})\right]^{0.8} \quad (6)$$

where δ_2^* is the boundary layer momentum thickness and V* is the velocity at the outer edge of the boundary layer for any surface point X = X* located in the turbulent boundary layer. If the momentum thickness at X = X* is perturbed by the amount $\Delta\delta_2^*$ the profile drag changes by

$$\Delta c_D = 2.41 \frac{\Delta\delta_2^*}{c} \left(\frac{\delta_2^*}{c_{D_p} \cdot c}\right)^{0.25} (\frac{V_*}{V_\infty})^{4.25} \quad (7)$$

Eq. 7 is also applicable to an airfoil on which the boundary layer momentum thickness is reduced by injecting high pressure air into the boundary layer. In this case a drag reduction is obtained that is considerably in excess of the thrust one would obtain if the high pressure air were discharged into the undisturbed freestream. Great care must however be taken that the injected high velocity air remains clear of the airfoil surface until it has mixed with the boundary layer air almost completely. Eq. 7 shows that for an airfoil with a roof-top velocity distribution, the largest thrust augmentation is obtained if the jet is discharged into the boundary layer immediately ahead of the pressure recovery region, since the product of $\delta_2^{*\,0.25}$ and $V_*^{\,4.25}$ is a maximum at this point.

The concept of the propulsive wing is analysed in detail in Ref. 7. It is shown there that for a lightly perturbed boundary layer, the ratio of profile drag reduction - ΔD_p by air injection to the reference thrust T_{Ref} produced by the same high-pressure air if it were discharged at a large distance from the airfoil, is given by

$$\frac{-\Delta D_p}{T_{ref}} = 0.95 (\frac{V_*}{V_\infty})^{2.25} \frac{\frac{V_{j_\infty}}{V_\infty}+1}{\frac{V_*}{V_\infty}(\frac{V_j}{V_*}+1)} \frac{\Delta\delta_{2_{jet}}}{\Delta\delta_{2_{ideal}}} \quad (8)$$

where V_* = velocity at the outer edge of the boundary layer at the station of discharge of the boundary layer jet

V_j = discharge velocity of the boundary layer jet

V_{j_∞} = discharge velocity of the reference jet

$\Delta\delta_{2\,ideal}$ = change of the boundary layer momentum thickness by the boundary layer jet if scrubbing losses are neglected

$\Delta\delta_{2\,jet}$ = change of the momentum thickness if scrubbing losses are included.

Eq. 8 was derived for the velocity profile shown in Fig. 8, with $X_k / C = 0.6$.

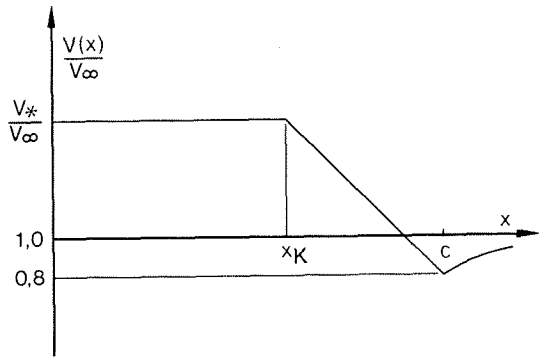

Fig. 8 Upper surface velocity distribution

$\Delta\delta_{2\,jet}$ is calculated as follows:

$$\Delta\delta_{2_{jet}} = \Delta\delta_{2_{ideal}} \left[1 - f\,(0.15+0.85\,V_*/V_j)\right] \quad (9)$$

where $(0.15 + 0.85\,V_*/V_j)$ is the ratio of the scrubbing losses incurred by a wall jet to its initial momentum thickness increment $\Delta\delta_{2_{ideal}}$ (see Ref. 8) and f is the ratio of the scrubbing losses of the boundary layer jet to the corresponding losses of the wall jet.

With the nozzle arrangement shown in Fig.9 it should be possible to keep the scrubbing losses well below 20% of the corresponding losses of a wall jet.

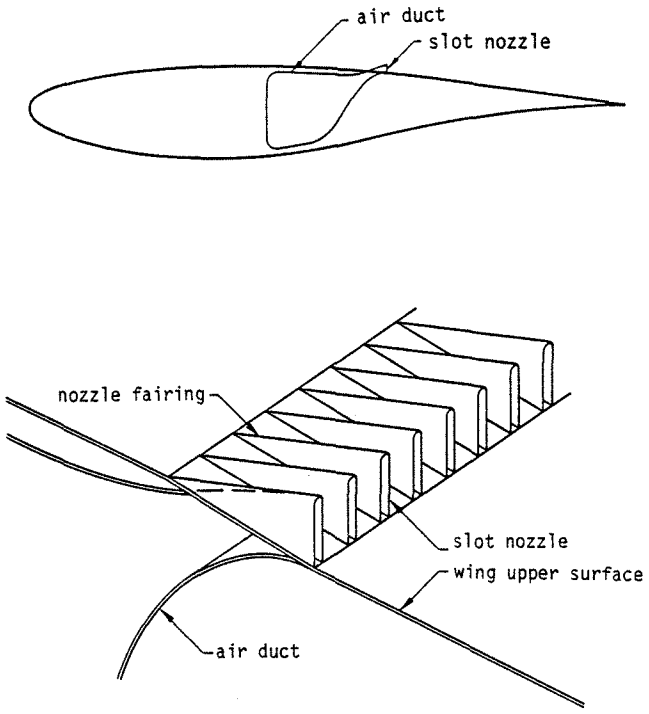

Fig. 9 Details of boundary layer slot nozzles

Fig. 10 shows the thrust augmentation ratio of a boundary layer jet as a function of the velocity at the outer edge of the boundary layer V_*/V_∞ and the jet velocity ratio V_j/V_* for f = 0.2 and $V_{j\infty}/V_\infty$ = 1.5. The latter value is representative for modern high by-pass ratio turbo-fan engines. In the limiting case of a very large nozzle exit area ($V_j/V_* \rightarrow 1.0$) thrust augmentation increases proportional to (V_*-V_∞), approximately. Also shown in Fig. 10 is the upper surface profile drag of a cambered airfoil with the roof-top velocity destribution shown in Fig. 8 referred to the upper surface drag of a flat plate of equal chord. These two results show quite clearly that the thrust augmentation achievable with the propulsive wing is directly related to the drag penalty that a thick profile has relative to a flat plate.

The decrease of thrust augmentation with an increase in jet velocity ratio essentially results from the decrease in the Froude efficiency of the boundary layer jet.

In Ref. 7 the special case of zero longitudinal force (thrust = drag) was also analysed on the assumption that the integral method for calculating the development of turbulent boundary layers can be applied to the boundary layer downstream of the jet exit, where δ_2 is negative. A further assumption was that the local skin friction coefficient $\tau_o/(\rho V^2)$ is constant between X_k and the trailing edge. The result of this analysis is shown in Fig. 11 for X_k/C = 0.6, f = 0.2 and V_j/V_∞ = 1.5. Comparing Fig.11 with Fig. 10, it can be seen that the thrust augmentation ratio decreases with the intensity of jet blowing.

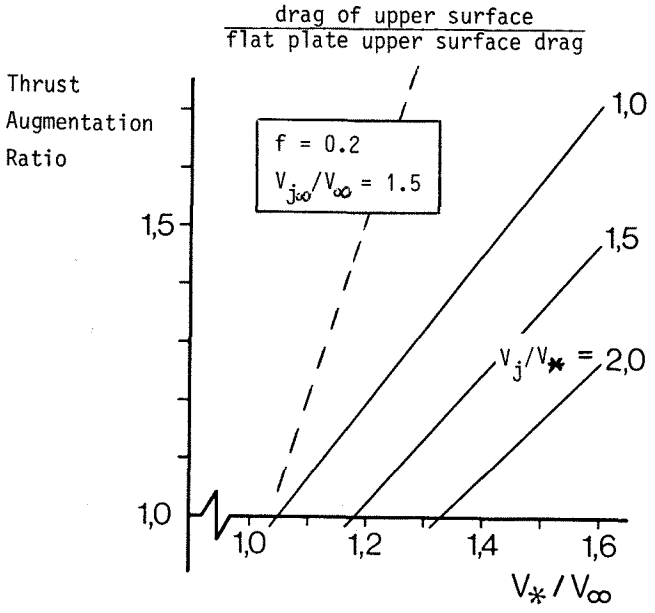

Fig. 10 Thrust augmentation ratio of a low-intensity boundary layer jet

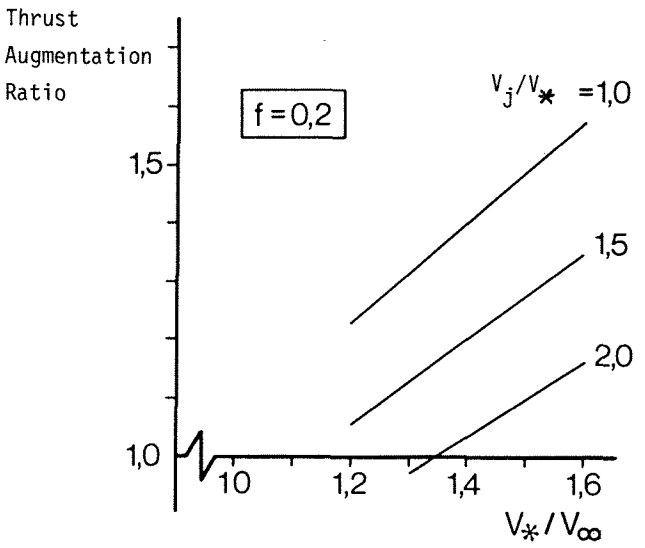

Fig. 11 Thrust augmentation ratio of a boundary layer jet for thrust = drag

The effectiveness of the concept of the propulsive wing cannot be quantified without wind tunnel tests for the following reasons:

- The analysis of Ref. 7 is restricted to incompressible flow. The effect of compressibility is not known.
- The applicability of the integral method to a boundary layer with a negative momentum thickness has yet to be demonstrated.
- The scrubbing losses of the nozzle arrangement shown in Fig. 9 - assumed to be 20% of those incurred by a wall jet - are not known.

Despite these uncertainties, the effectiveness of the propulsive wing shown in Fig. 12 was assessed for the case thrust = drag and plotted in

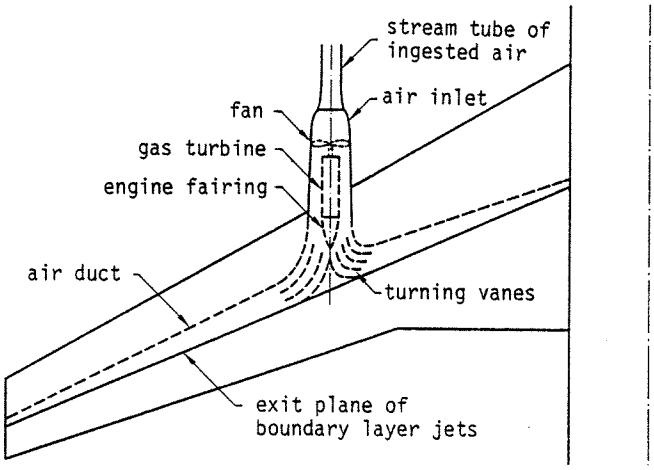

Fig. 12 General arrangement of propulsive wing

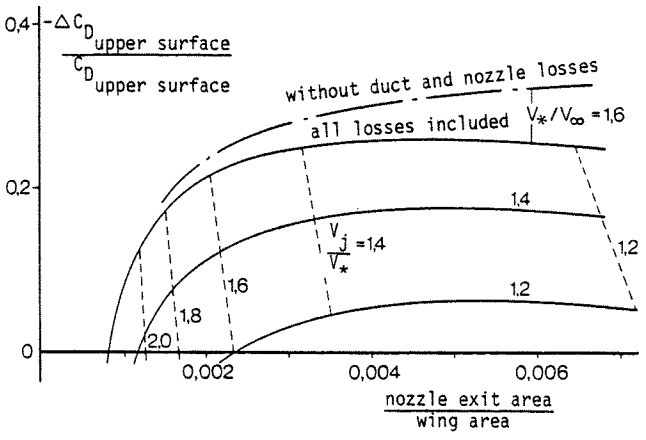

Fig. 13 Relative upper surface drag reduction due to boundary layer blowing

Fig. 13 as a function of the nozzle exit area ratio for three values of V_*/V_∞. It can be seen that if the duct and nozzle losses are included, there exists an optimum nozzle area ratio at which thrust augmentation is maximised.

A value of $V_*/V_\infty = 1.5$ is representative of the upper surface velocity of modern transport aircraft in cruising flight. Assuming that on a propulsive wing advantage would be taken of the boundary layer energising action of the jet and V_*/V_∞ would be increased to 1.6 by increasing the wing thickness or reducing the wing area, a thrust augmentation of 26% of the upper surface wing drag would be obtained. Further thrust augmentation is possible if the nozzle flow is increased further.

For highly loaded wing sections the upper wing surface provides about 75% of the wing profile drag. The latter, again, makes up approximately 25% of the aircraft cruise drag, so that the propulsive wing could possibly reduce the fuel requirement of transport aircraft by approximately 5%. The positive effect of boundary layer energising on $C_{L\ max}$ and $C_{L\ buffet}$ and the negative effect of the weight and volume of the air ducts are not included in this figure.

5. Reduction of Induced Drag by Means of Multiply Bifurcated Wing Tips

It is well known that the induced drag of a wing can be reduced by adding one or more coplanar or non-coplanar winglets to the wing tips. The formula for the vortex drag of an elliptically loaded plane wing

$$D_{vortex} = \frac{(L/b)^2}{\pi q} \qquad (10)$$

shows that the drag reduction essentially stems from a reduction of the mean aerodynamic force per meter of total projected wing length. Alternatively, the winglets can be viewed as sails developing a normal force that is tilted forward as a result of the local cross-flow velocity.

It is surprising that the associated problem of the effect of winglets on wing weight has received little attention in the past. In Ref. 9 the aerodynamic effectiveness of the various non-planar wing tip configurations was investigated on the basis of constant-weight wings. Each non-planar wing was sized in such a way that the wetted area, the thickness-to-chord ratio, and the quantity

$$W = \int_{y_{root}}^{y_{tip}} \frac{\text{bending moment}}{\text{wing thickness}}\, dy \qquad (11)$$

were the same as the corresponding values of a plane reference wing with an elliptical span loading. For the non-planar wings a minimum-drag lift distribution was also stipulated. The assumption was

that wings having equal values of the above three quantities have the same weight. It was found that all non-planar wings have a smaller wing span than the plane reference wing of equal weight.

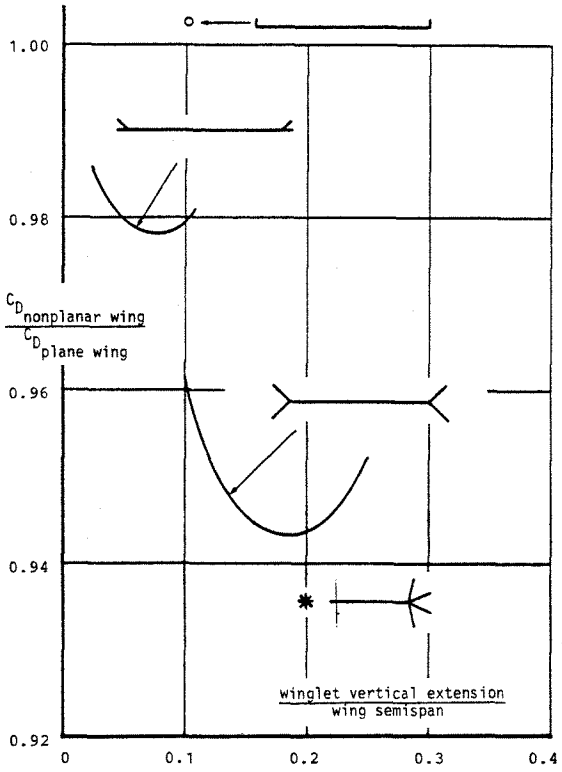

Fig. 14

Fig. 14 shows the vortex drag of three types of non-planar wings referred to the vortex drag of the equal-weight plane wing as a function of the relative winglet size. The distance from the tip of the winglet to the wing plane referred to the wing semi-span was used as a measure of winglet size, because the calculations had shown that the vortex drag is determined primarily by this parameter. The lower curve applies to the symmetrically bifurcated wing tip with 45° dihedral angle. It can be seen that the vortex drag initially decreases with increasing winglet size, passes a minimum at a winglet span of 25% wing semi-span, and increases again as a result of the rapidly decreasing span of the rescaled non-planar wing.

In a previous calculation, the dihedral angle of 45° had been shown to be optimal. With this wing tip configuration the vortex drag can be reduced by 5,6% relative to that of the equal-weight plane wing.

The upper curve of Fig. 14 applies to unsymmetrically bifurcated wing tips for which one winglet has 45° dihedral and the other is co-planar with the wing. As can be seen, any deviation from the symmetrical configuration results in a sharp increase in effective induced drag and requires a smaller winglet for the minimum-drag design.

In Fig. 14, the open circle applies to a single winglet with a span of 10% wing semispan with zero cant angle. This result shows that no real drag benefits can be expected from single-winglet wing tip designs.

The effective drag of a non-planar wing with four winglets per wing tip and dihedral angles of $\pm$ 17° and $\pm$ 50° is shown in Fig. 14 by the star symbol. As can be seen, the additional aerodynamic benefit is almost completely compensated by the weight penalty of the multiply forked tip relative to the bifurcated wing tip. This result shows that there is little incentive to add more than two winglets per wing tip.

Since wing tip bifurcation results in a reduction of the effective vortex drag of a wing, it may be conjectured that bifurcation of the winglets provides a further reduction of the effective vortex drag. Such a doubly bifurcated symmetrical wing tip was also investigated. Drag optimisation is more laborious since there are five free parameters in this case - inner winglet size and dihedral as well as outer winglet size and dihedral (two angles).

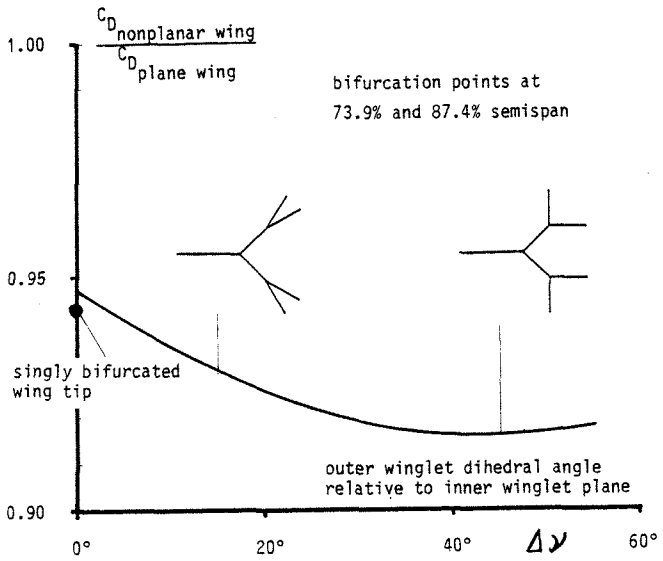

Fig. 15 Influence of outer winglet dihedral angle on effective vortex drag of wings with doubly bifurcated tips

Fig. 15 shows the effective vortex drag for a doubly bifurcated wing tip with bifurcation points at 73.9% and 87.4% wing span and an inner winglet dihedral angle of 45°. $\Delta\nu$ is the dihedral angle of the two outer winglets relative to the inner winglet plane. For $\Delta\nu$ = 0 the effective vortex drag is a little higher than that of the twin-winglet tip because of the reduced wing thickness in the region of the outer winglets. Unfolding of the outer winglets reduces the effective vortex drag

until a maximum drag reduction of 8.5% is reached at $\Delta\nu = 42°$.

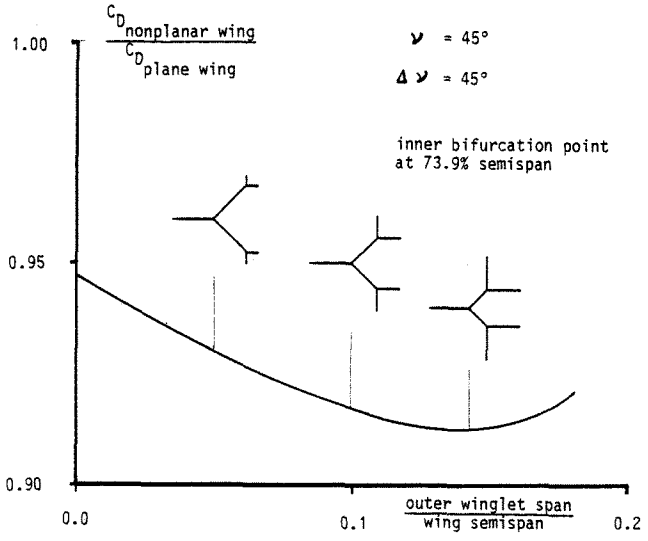

Fig. 16 Influence of outer winglet size

Fig. 16 shows the effect of outer winglet size on vortex drag for $\nu_i = 45°$ and $\Delta\nu = 45°$. A minimum effective vortex drag of 91.2% is provided by an outer winglet span of 14% wing span.

Finally, in Fig. 17 the effect of rotating the outer winglet pair through an angle $\Delta\nu'$ is shown. It is interesting to note that even in this unsymmetrical situation symmetrical bifurcation of the two winglet tips provides the highest drag reduction.

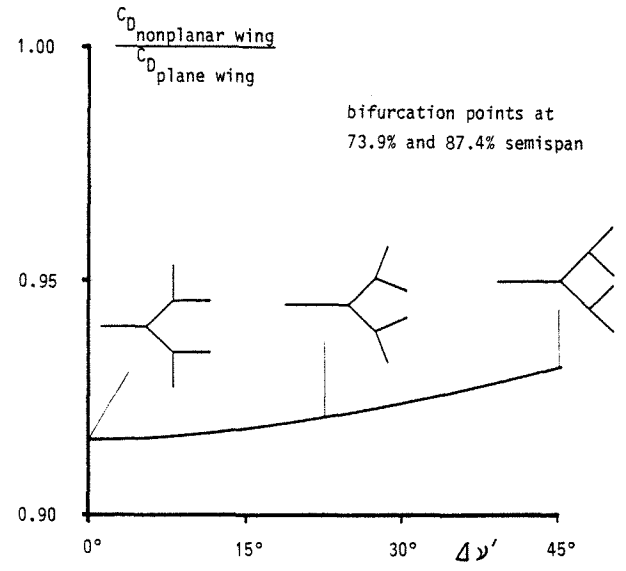

Fig. 17 Influence of outer winglet asymmetry on effective vortex drag of wings with doubly bifurcated tips.

Fig. 18 shows the minimum-drag normal force distribution for the optimum doubly bifurcated wing tip in comparison to the elliptical distribution form of equal lift.

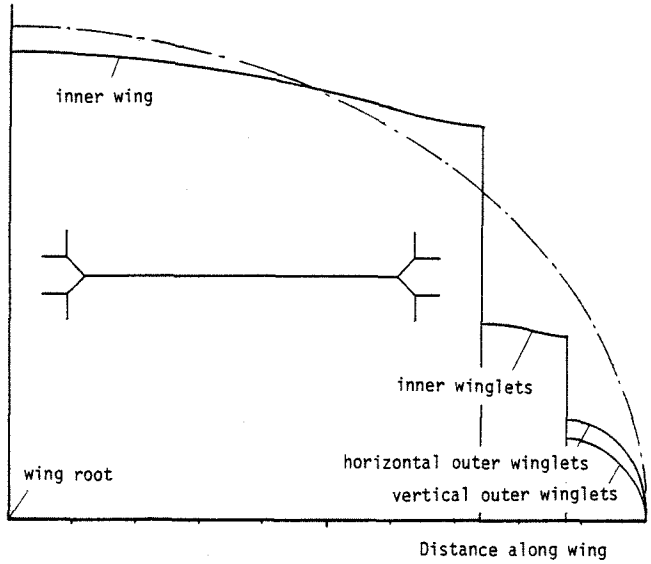

Fig. 18 Minimum-drag normal force distribution of optimum non-planar wing with doubly bifurcuted tips

Summing up, single-winglet and unsymmetrical twin-winglet wing tip configurations are of limited drag benefit if the increased wetted area and bending moments are taken into consideration. With single symmetrical wing tip bifurcation an effective vortex drag reduction of 5,6% can be obtained while double bifurcation leads to a drag reduction of 8,8%. It is to be expexted that triple bifurcation would provide a further drag reduction.

For long range transport aircraft, the vortex drag makes up approximately 30% of the total aircraft drag in cruising flight. With doubly bifurcated wing tips the fuel consumption could be reduced by some 3%.

6. Reduction of Induced Drag by Means of Freely Floating Tip Vortex Sails

The non-planar wing is heavily penalised by the weight increment resulting from the higher wing bending moments. For example, the symmetrically bifurcated wing tip with a winglet span of 25% wing semi-span and 45° dihedral angle (the optimum twin-winglet wing of Fig. 14) provides a vortex drag reduction of 23% relative to the plane wing of equal span. This benefit falls to 5,6% when the comparison is made on an equal-weight basis. It would therefore be desirable to have a device that reduces vortex drag at cruise without loading the wing more than is necessary.

Such a device is shown in Fig. 19. At the aft end of a

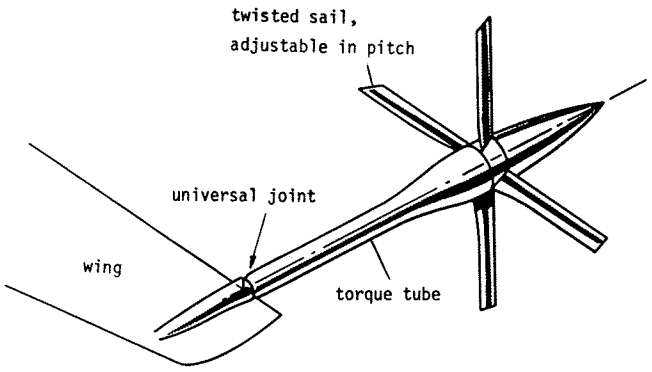

Fig. 19 Sketch of freely floating tip vortex sails

torque tube that is connected to the wing tip by means of a universal joint are mounted a number of sails with which a large proportion of the tip vortex swirl is removed in cruising flight. Upon a change of angle of attack or side slip the trailing unit floats into a position that is free of a pitching and yawing moment about the universal joint. The sails are mounted in the hub in such a way that their pitch angle can be changed by means of a mechanical linkage that passes through the torque tube and is attached to the wing tip eccentric to the universal joint. The gearing ratio of this linkage is designed so that upon a change in angle of attack the sail pitch angles change in such a way that their angle of attack relative to the rotating tip vortex flow remains essentially constant.

With such a device, only the torque resulting from the derotation of the tip vortex flow in cruising flight is applied to the wing. In contrast to wing tip mounted winglets this moment does not increase with load factor and practically no lift or side forces are applied to the wing.

It is estimated that the fuel consumption of transport aircraft can be reduced by some 2% with such free-floating, geared tip vortex sails. Clearly, sail tip bifurcation would increase the effectiveness of such a device.

7. Conclusions

As a result of the dramatic increase in fuel price in the past decade, aircraft drag has become the decisive factor in the determination of the operating costs of transport aircraft. In this paper, the following five new concepts for reducing aircraft drag are proposed:

- Active boundary layer thickening to reduce fuselage skin-friction drag.
- Low pressure jet mixing to augment engine thrust.
- The propulsive wing to reduce wing profile drag.
- Multiply bifurcated wing tips to reduce wing vortex drag.
- Freely floating tip vortex sails to reduce wing vortex drag.

Each concept presents a number of new, interesting and challenging tasks to the design aerodynamicists. Application of these concepts to long range transport aircraft could reduce the total fuel burn by some 20% relative to the current generation of turbo-fan powered transports.

8. References

(1) Löbert, G.: Drag reduction by means of active boundary layer thickening. 23rd Israel Annual Conference on Aviation and Astronautics, Tel-Aviv, Feb. 11, 1981.

(2) Williams, M.R.: Large turbo-fans to the year 2000. Aeronautical Journal, Jan. 1984, pp. 419-426.

(3) Stewart, D.J. and Campion, B.S.: New technology in commercial aircraft design for minimum operating cost. J.Aircraft, Vol. 17, May 1980, pp. 365-371.

(4) Ewald, B.: Engine jet simulation problems in wind tunnel tests. AGARD Conf. Proc. 150 (1974), pp. 26-16 to 26-32.

(5) Löbert, G.: Theorie der Widerstandsinterferenz von Tragflügel und Triebwerksstrahl. Z.f. Flugwissenschaften u. Weltraumforschung, Vol. 6 (1982), Heft 6, pp. 433-440.

(6) Schlichting, H.: Boundary-Layer theory. McGraw-Hill Book Company, New York, 1968

(7) Löbert, G.: Verringerung des Kraftstoffverbrauchs von Transportflugzeugen durch Strahlausblasung am Flügel. MBB Technical Note FE115-82, Aug. 11, 1982.

(8) Thomas, F.: Untersuchungen über die Erhöhung des Auftriebes von Tragflügeln mittels Grenzschichtbeeinflussung durch Ausblasen. Z.f. Flugwissenschaften, Vol. 10 (1962), Heft 2, pp. 46-65.

(9) Löbert, G.: Der Flügel mit Gabelspitzen als Mittel zur Erhöhung der Wirtschaftlichkeit von Transportflugzeugen. DGLR Paper 77-017, DGLR Annual Conferenze, Berlin, Sept. 15, 1977.